ABSTRACT

INVESTIGATION OF THE POTENTIAL CATALYTIC ACTIVITIES OF SEVERAL METAL ORGANIC FRAMEWORK (MOF) MATERIALS

by
Guangyu Zhang

Metal-organic frameworks (MOFs) are promising porous materials due to their high porosities, large apparent surface areas, tunable pore properties and selective uptake of small molecules. Many researches have been focused on developing new MOF structures and exploring their use in gas storage and separation. Only few studies investigated the catalytic properties of MOFs. In this study, catalytic properties are explored over several MOFs including zeolitic imidazolate framework-8 (ZIF-8), Ni(FA) and Zn(FA). These MOFs are used as catalyst supports for iron or platinum nanoparticles. The catalysts are prepared using incipient wetness impregnation method and characterized with Brunauer-Emmett-Teller (BET), pulse chemisorption, X-ray diffraction (XRD), temperature-programmed reduction (TPR), and temperature-programmed desorption (TPD). The catalysts are tested from the water gas shift and methanol oxidation reactions using a fixed bed flowing reactor at 1 atm. The characterization results show that these MOFs decompose at relatively low temperatures. These materials did not have good activities for the water gas shift reaction under the operation conditions. Based on the methanol TPD results, Pt-ZIF8 showed some methanol oxidation activity. The low activity is possibly due to the low operation temperatures since the operation temperatures are limited by the stability of the MOF materials. This pioneering work indicates that it is critical to improve the stability of the MOFs during catalyst preparation and under the reaction conditions for their application in catalysis field.

INVESTIGATION OF THE POTENTIAL CATALYTIC ACTIVITIES OF SEVERAL METAL ORGANIC FRAMEWORK (MOF) MATERIALS

by
Guangyu Zhang

A Thesis
Submitted to the Faculty of
New Jersey Institute of Technology
in Partial Fulfillment of the Requirements for the Degree of
Master of Science in Chemical Engineering

Otto H. York Department of
Chemical, Biological and Pharmaceutical Engineering

May 2011

Blank Page

APPROVAL PAGE

INVESTIGATION OF THE POTENTIAL CATALYTIC ACTIVITIES OF SEVERAL METAL ORGANIC FRAMEWORK (MOF) MATERIALS

Guangyu Zhang

Dr. Xianqin Wang, Thesis Advisor   Date
Assistant Professor of Chemical, Biological and Pharmaceutical Engineering, NJIT

Dr. Zafar Iqbal, Committee Member   Date
Research Professor of Chemistry and Environmental Science, NJIT

Dr. Kamalesh K Sirkar, Committee Member   Date
Distinguished Professor of Chemical, Biological and Pharmaceutical Engineering, NJIT

BIOGRAPHICAL SKETCH

Author: Guangyu Zhang

Degree: Master of Science

Date: May 2011

Undergraduate and Graduate Education:

- Master of Science in Chemical Engineering,
  New Jersey Institute of Technology, Newark, NJ, 2011

- Bachelor of Science in Chemical Engineering,
  Jiangsu Polytechnic University, Changzhou, P. R. China, 2009

Major: Chemical Engineering

To my beloved family and especially my girlfriend Catherine for their love,
encouragement and support

ACKNOWLEDGEMENT

TABLE OF CONTENTS

TABLE OF CONTENTS
(Continued)

LIST OF TABLES

LIST OF FIGURES

CHAPTER 1

INTRODUCTION

In the past decade, metal-organic frameworks (MOFs), as a novel class of porous materials, have attracted widespread attention due to their high porosities, large apparent surface areas, tunable pore properties and selective uptake of small molecules[1]. These attributes make MOF materials promising in many applications such as gas storage and separation, catalysis, optical sensors and emerging drug delivery[2]. Most of MOFs possess three-dimensional crystalline structures and well-defined pores with uniform sizes. The assembly of MOF structure is realized by periodic duplications of molecular secondary building units (SBUs), which are built by linking organic ligands with metal ion clusters that act as inflexible centers[1].

Zeolitic imidazolate frameworks (ZIFs), as a subsidiary of metal-organic frameworks, combine the properties of both MOFs and zeolites including zeolite-like topology, high porosity, tunable pore properties and excellent chemical stability. ZIFs employ the topology of aluminosilicate zeolites: tetrahedral Si (Al) and the bridging oxygen atoms are substituted with transition metal ions (usually Zn^{2+} or Co^{2+}) and imidazolate links, respectively. In the ZIF structure, transition metal ions are uniquely coordinated with the nitrogen atoms of imidazolate links at the angle of approximately 145°, which agrees well with the Si-O-Si angle in zeolites. In contrast to other MOFs, ZIFs have exceptional chemical stability in water and organic solvents, which makes ZIFs attractive in industrial large-scale production. Currently, ZIFs have also been developed in gas storage and separation like selective uptake of carbon dioxide[3].

1.1   Synthesis of MOFs

Reticular synthesis is used to exploit the design and assembly of MOF structures, in which SBUs are held together by strong coordination bonding. The primary goal of reticular synthesis is to achieve the predetermined structure and obtain the expected functionalities. Usually, the MOF network is constructed by establishing metal-organic bonds and a desired SBU is expected to generate in situ, maximizing the voiding space within the framework. The properties of metal clusters and organic ligands determine the functionality of as-synthesized MOFs, such as porosity, porous size, porous surface and other physical properties. Besides, the synthesis of MOF relies on solvent polarity, PH value of solution, reaction temperature and mole ratio of starting materials[4].

Although a large number of MOFs with diverse structures were synthesized, only a small number of simple, highly symmetric inorganic SBUs were adopted. For example, the cubic diamond network represents the simplest, the highest symmetry, and the unique regular tetrahedral structure[5]. To obtain robust MOF frameworks, it is not only building blocks that are important, but also the way in which they are connected together. The expansion of these inorganic SBUs is achieved by linear rigid organic linkers that define the voiding space within the framework.

Here three synthetic strategies are introduced to improve the porosity and achieve large pore sizes of MOFs[4]: (1) Designing the inorganic and organic four-connected building blocks with zeolite-like topology: the structure of MOFs with expanded zeolite topology would have larger pores and higher porosity than zeolites. (2) Replacing a vertex in a network with larger metal clusters would expand the size of inorganic SBUs and the dimension of the network, which leads to large pore size and high porosity. (3) Employing

larger and longer organic ligands would expand the length of linkers between building blocks, benefitting large pore diameter and high porosity.

The common crystal lattice growth methods include solvent evaporation, diffusion, solvothermal method, microwave and ultrasonic technique[4]. These methods generally involve slow introduction of the building blocks to reduce the rate of crystallite nucleation.

Solvent Evaporation Method: Solvent evaporation is a traditional and commonly used crystal growth method by evaporating or cooling a solution, usually requiring two convenient conditions: (1) crystal growth in saturated solutions; (2) solubility increases with temperature and crystals can appear during the cooling step.

Diffusion Method: The principle of this technique is to slowly bring into contact the different species. One approach is solvent liquid diffusion by forming two solvent layers with different densities. One contains the product in a solvent; another is the precipitant solvent, and these are separated with a solvent layer. The precipitant solvent slowly diffuses into the separate layer and crystal growth occurs at the interface. The other approach is the slow diffusion of reactants by the separation of physical barriers, such as two vials with different sizes. The diffusion method is preferred to produce single crystals suitable for X-ray diffraction analysis, instead of non- or poly-crystalline products, especially if the products are poorly soluble.

Solvothermal Method: Solvothermal technique has been regarded as the most common synthetic method for MOFs so far. It exploits the self-assembly of MOF structures from soluble precursors: usually heating a mixture of organic species and metal salts in an amide solvent (such as DMF) at the temperature range of 80-260 ˚C for 12-48 h.

Also, a volatile amine is slowly added as base during the reaction to deprotonate the organic linkers, which are subsequently coordinated with vacant metal sites.

This method often yields high quality crystals suitable for single crystal X-ray diffraction analysis, but has the obvious disadvantage of being relatively slow (hours to weeks). If a high yield is desired over crystal quality, reaction time can be greatly reduced by increasing the reactant concentration and the agitation of solution. However, solvothermal conditions are not applicable to thermally sensitive organic ligands.

Microwave Heating: Recently, microwave heating has been employed as an alternative of conventional heating for synthesis of crystalline MOFs. The mechanism is to enhance the rate of chemical reactions in microwave-absorbing solvents, which absorb microwave irradiation and generate high temperatures instantly. Either of the rate of nucleation and the rate of crystal growth is promoted in this high speed synthesis (only several minutes required). In addition to the fast reaction time, microwave heating is also a good way to control the size and the shape of the resulting particles by varying the precursor concentrations.

So far, it is still a major challenge to explore successful synthetic strategies for MOFs, in order to obtain the expected structures and functionality. Furthermore, the control of dimensionality in the MOF structure is another challenge to overcome. A term "catenation" is necessary to be introduced. It is defined as where two or more identical frameworks are inter-grown at the expense of pore volume. There are two forms of catenation[5]: (1) interpenetration, where the networks are maximally superposed from each other; (2) interweaving, where they are minimally occupied and exhibit close contacts

that may result in mutual reinforcement. The former is usually one of the major obstacles, which decrease the dimensionality of porous MOF structures.

1.2   Applications

Compared to traditional porous materials, MOFs exhibit more flexible tailoring of their pore properties like pore dimensions, shapes, sizes and pore surface. Most of MOFs have uniform pores with tunable sizes and a network of channels. These pores and channels are often filled with terminal ligands and guest species such as water and/or organic solvents. Removal of these guest molecules often results in framework collapse; however, in many cases, the integrity of framework is well-maintained, and these voids remain available for adsorption of other guest molecules.

In the MOF structure, SBUs decorate the nodes and expand the inorganic topology, which gives them remarkably high surface area and porosity as well as uniform pore size due to their crystalline state. Through removal of the terminal ligands, two classes of well-defined molecular adsorption sites within MOF structure are formed: unsaturated metal centers (UMC) and guest-accessible functional organic sites. These porous features lead MOFs to a wide range of applications, but the major function of MOFs is to behave as hosts for storing certain molecules and/or supporting embedded functional particles depending on their shapes and sizes[4].

The structural stability of MOFs in aqueous solution should be carefully studied. Water stability is an essential property for porous carriers that have potential in industrial applications as moisture is usually present in at least small amounts. The water stability of MOFs is relative to several factors including the metal clusters, metal-ligand bond strength and oxidation state of the metal. The liability of metal-oxygen bonds in carboxylate MOFs,

such as MOF-5, results in hydrolysis of their networks thus irreversibly destroying their structures. Zeolitic imidazolate frameworks are composed of imidazolate or related linkers, which greater basicity as compared to typical carboxylate linkers results in stronger metal-nitrogen bonds thereby better resistance to hydrolysis[6]. In addition, most of industrial practices require a certain stability towards moisture in order to facilitate handling and thus to reduce production costs[7].

Energy Storage: As increasing environmental issues were brought by combustion of fossil fuels, the exploration of more effective and environment-friendly energy sources have been attracting much attention. Among a variety of alternative fuels, hydrogen and methane have been recognized as ideal energy sources due to their clean combustion and high heating values. However, hydrogen and methane are both volatile gases under ambient conditions. Effective storage and safe delivery of them becomes the key elements of industrial applications. MOF as a novel kind of porous materials with high porosity, uniform and tunable pore size as well as functional pore surfaces rapidly becomes a candidate of hydrogen and methane storage materials.

The breakthrough in lightweight hydrogen storage will significantly provide a new energy carrier in transportation sector. The transportation sector represents the largest consumer of oil, thus making it one of the largest sources of airborne pollutants such as carbon and nitrogen oxides. The U.S. Department of Energy (DOE) has projected the current target with the concept that today's vehicles will be powered by tomorrow's higher efficiency fuel-cell power sources[8].

Coupled with measurements of porosity based on nitrogen adsorption, many methods have been developed to obtain a detailed understanding of the hydrogen

adsorption sites within MOF structure. Neutron diffraction and infrared spectroscopy have been used to explore the site-specific interactions of hydrogen within a framework and the energies of those binding events. In addition, computational modeling of MOF structures and hydrogen adsorption has been emerging in recent years. For instance, gas adsorption isotherms and diffusion coefficients can be obtained from grand canonical Monte Carlo (GCMC) and molecular dynamics (MD) simulation, respectively[2]. These simulation methods can be used as a predictive tool in the development of MOFs for specific applications.

Traditional hydrogen storage materials, such as carbon-based materials or metal hydrides, have higher temperature need for hydrogen desorption, low gravimetric hydrogen contents, problems associated with their regenerations, costs, susceptibility to contamination caused by impurities. MOFs exhibit exceptional hydrogen uptake by mass but are also characterized by very weak adsorption energies (typically 4-10 kJ/mol), such that cryogenic temperatures are required to achieve significant hydrogen storage[4].

Several design principles have been proposed to increase the hydrogen storage properties in MOF frameworks[4]: (1) High framework porosity is necessary for high hydrogen saturation uptake. (2) The enthalpy of adsorption is also greatly dependent on the size of the pore. Narrow pores actually take up hydrogen more efficiently than very large ones. Hence, catenation and interpenetration networks are designed for hydrogen storage. (3) Partial charges, either positive or negative, on the MOF surface can provide a means of strengthening the binding of hydrogen through dipole-induced dipole interactions. In particular, the introduction of open metal sites into MOF is considered one of the most effective means of increasing adsorption enthalpy of hydrogen. In addition to hydrogen,

methane is another effective alternative fuel to replace gasoline and diesel fuels in vehicular applications. The hydrogen storage strategies, such as high porosity and appropriate pore size, can be equally applied to methane storage.

Separation: One of the major applications of porous materials is separation of mixtures of gases or liquids, such as purification of O_2 and N_2, removal of volatile organic compounds, and separation of CO_2 from CH_4 in natural gas. Separation relies on two mechanisms: thermodynamic, by which one component is selectively adsorbed over others in the mixture and kinetic, by which separation relies on the path the components take through the pores of the material. MOFs as a novel class of porous materials allow their pore textural properties to be systematically tuned by the appropriate choice of metal and ligand constituents and synthesis approach, which makes them potentially useful in molecular separation.

One of the advantages of MOFs for gas or liquid separation is the functionality of their pore surface, through which the two similar gases can be separated. For example, C_2H_2 and CO_2 are similar in equilibrium sorption parameters, related physicochemical properties, and molecular size and shape, hence hard to separate. The separation was realized by employing the functionalized surface of a MOF, Cu_2(pyrazine-2, 3-dicarboxylate)$_2$(pyrazine), which exhibited a high level of selective uptake of C_2H_2 molecules compared to CO_2 molecules[4]. In addition, pore size also plays a key role in adsorption levels, with the best interactions found when the pore closely matched the size of the adsorbate.

The use of MOFs for separation is also advanced in the integration of MOFs into membranes. Membrane-based technologies have been widely applied on an industrial

scale to gas separation. Membranes rely on a permeability differential between two gases, based on pore size and shape and chemical functionality. As these are tunable properties in MOFs, more so than in zeolites or other porous materials, they represent a promising new material class for separation membranes. Porous crystalline materials, such as MOFs, can obviate the tradeoff between selectivity and throughput that is often found in polymeric membranes. MOFs can either be integrated into a polymer matrix or grown directly as thin films[2].

Catalysis: In the past decade, the use of MOFs as solid catalysts has attracted much attention, because the pore size and functionality of the structure can be adjusted for a variety of catalytic reactions. Coupled with their nanoporosity, the inorganic-organic hybrid nature of MOFs provides multiple opportunities to create one or more catalytic sites within a pore. Most of MOF catalysts rely on the framework metal, especially the unsaturated metal sites. Although a large number of MOFs are known, only a few of them have been tested in catalytic reactions so far. It is still a challenge to find out whether the metal centers, the functionalized ligands, or even metal-ligand interactions or differences in particle size, can cause unusual catalytic properties[4].

MOF pores can also serve as hosts for guest molecules or as templates and supports for metal nanoclusters. Due to their extraordinary high surface areas and well defined porous structures, MOFs can be used for the stabilization of embedded metal particles with adjustable sizes. The included metal particles are still accessible for other reagents due to the high porosity and huge voids in MOFs. This fact makes "metal/MOF" systems especially attractive in the field of heterogeneous catalysis. Here three techniques of preparing these systems are introduced[9].

Chemical Vapor Deposition (CVD): Volatile organic metal precursors are introduced into the MOF pores or channels by a sublimation process in the absence of solvents. This solvent-free method avoids some deficiencies of liquid-phase impregnation of MOFs with guest molecules that are typically dissolved in organic solvents. After incorporation of vapor precursors, the included metal precursors are thermally or photochemically decomposed and further reduced to active metal particles. The absence of solvent molecules during the gas-phase infiltration process allows an extremely high metal loading up to 30-40 wt% in a single loading step. The drawback of such high loading levels is the agglomeration of nanoparticles and partial or even full degradation of the MOF in case of high reactive particles (i.e. palladium (Pd)). Besides, the ultrahigh metal loading is not in favor of an optimal metal dispersion on the supported MOF. Several metal/MOF systems were synthesized using CVD method, such as Pd/MOF-5[10].

Incipient Wetness Impregnation: The simplest and the most common procedure for depositing metal nanoparticles onto MOF supports is the use of an aqueous or non-aqueous solution containing a metal salt for liquid impregnation. After incorporation of metal salt precursors, the included precursor/MOF samples are calcined and further reduced to the specific metal/MOF systems. The liquid impregnation is relatively easy to operate, although it is less efficient in metal loading than CVD. For use in heterogeneous catalysis, high metal loadings are not required, usually 1-5 wt% of active metals are sufficient. Hence incipient wetness impregnation is an effective catalyst preparation method, avoiding the use of highly reactive and air sensitive precursors in CVD. This method is generally limited by the solubility of the selected precursor in suitable solvents. In aiming at higher metal loadings, removing the solvent in the case of incipient wetness impregnation may cause

problems in terms of segregation of the precursor molecules to the outer surface of the MOF crystallites, which is favored by capillary forces.

Solid Grinding: The deposition of metal nanoparticles onto MOF supports can also be achieved by solid grinding of a volatile precursor together with an activated MOF material. This method was especially developed for supporting nanosized gold clusters on different MOF materials, such as Au/ZIF-8[11]. Essentially, the solid-grinding method is similar to chemical vapor deposition, because the chosen precursors are volatile and may be absorbed from the gas phase into the MOF structure during the grinding process. This method is a simple and effective way of producing nanosized metal particles without solvent and washing procedures after deposition.

All the different systems and preparative procedures have a number of common aspects and in particular share the issues of nonselective deposition at the outer surface of the MOF support versus loading the cavities inside the bulk phase, control of the size distribution and the formation of particles of a size exceeding the MOF cavities, framework degradation during nanoparticle formation, control of the particle size distribution, and so on. Actually, achieving a high loading of MOFs with cavity-size-matched metal particles and a homogeneous dispersion throughout the bulk of the MOF matrix is a nontrivial target both for the synthesis and characterization of the obtained microstructure and for ruling out any artifacts[9].

So far all reported metals/MOFs cases can be categorized into three classes[9]. Class A contains the cases in which the metal nanoparticles were deposited preferentially at the outer surface of a MOF crystal or close to it and exhibit a particle size substantially larger than the accessible pore dimensions. Particles distributed throughout the volume of the

MOF crystal but still exhibiting a broad size distribution with a particle size characteristically larger than the dimensions of the pores are assigned to class B. Particles distributed throughout the MOF crystal and exhibiting an average particle size matching the pore dimensions are regarded as class C.

The formation of metal nanoparticles may be accompanied by a partial or even full degradation of the MOF. It is assumed that initially many small nuclei are formed, which rapidly agglomerate in the case of a very weakly interacting (stabilizing) framework until a certain point is reached where no other feed particles are available in the direct environment of the formed bigger nanoparticles. This explains the observed in-homogeneity of the loading when MOF systems with 3-D pore structure and large windows between the pores are used. The diffusion of performed small nanoparticles inside MOFs can be decreased by using frameworks with directed porosity where the single pores are not connected to each other[9].

Drug Delivery: With their tunable host-guest and facile modification via chemical synthesis, MOFs represent a very attractive platform for drug delivery systems. Currently, a large portion of the recent work in the field of MOF drug delivery is focused on MIL compounds. One group very recently published a more comprehensive study of drug delivery with MIL nanoparticles in which they considered an array of five frameworks and nice drugs[2]. Furthermore, in vitro cell studies and in vivo rat studies demonstrated the low toxicity of these Fe MOF nanoparticles. These results underline the promise of MOFs in this filed and indicate that MOFs are ready for more extensive biological testing as drug carrier.

1.3 Several Typical MOFs

Here several landmark MOF materials are introduced because they represent a wide range of desirable structures and functionality such as ultrahigh surface area and porosity (MOF-5 and MOF-177), open unsaturated metal sites (HKUST-1) and exceptional chemical stability (MIL-101 and ZIF-8). These attributes have significant implications in high storage capacities of gas molecules and other applications.

MOF-5: Yaghi and coworkers initially synthesized the prototype of MOF materials, MOF-5. Standing out of a variety of known MOFs, MOF-5 [$Zn_4O(bdc)_3$, bdc= benzene-1, 4-dicarboxylate, also $Zn_4O(C_8H_4O_4)_3$] is one of few truly robust frameworks without collapse in the absence of guest molecules. The MOF-5 structure is built by linking inorganic Zn_4O^{6+} clusters with rigid linear carboxylate linkers. The apparent Langmuir surface area of MOF-5 (assuming monolayer coverage of N_2) was estimated at 2900 m^2/g, as well as a free porous volume 1.04 cm^3/g or 0.61 cm^3/cm^{3}[12]. However, it is considered as sensitive to moisture when exposed to air and unstable in water due to the liable metal-ligand bonds mentioned above.

MOF-177: With the formula of $Zn_4O(btb)_2$ (btb= benzene-1, 3, 5-tribenzoate), MOF-177 has an extremely high Langmuir surface area over 5000 m^2/g and a significant uptake of hydrogen under the condition of high pressure and low temperature: gravimetric density up to 7.5 wt% at 77 K and 70 bar. Due to its large pore sizes and huge central voids, MOF-177 makes the incorporation of other functional particles available thus provide more adsorption sites for gas molecules. For example, the incorporation of platinum nanoparticles into the MOF-177 structure has been developed in hydrogen storage and heterogeneous catalysis[13, 14].

HKUST-1: HKUST-1 [$Cu_2(btc)_3$, btc= benzene-1, 3, 5-tricarboxylate] is a copper-based MOF material, featuring in three-dimensional crystalline structure with square-shaped pores (9 Å ×9 Å in cross section). In the center of HKUST-1 structure, each of divalent copper atoms is coordinated by four oxygen, giving $Cu_2C_4O_8$ cages. The unsaturated metal centers, also known as open metal binding sites are basically formed after the removal of water molecules. The free sites of unsaturated Cu^{2+} become available for additional gas molecules. The combination of open metal sites and the net topology exhibits promising adsorption properties in hydrogen storage and gas separation (NO_X and CO_2 traps)[15]. The stability of HKUST-1 was also measured at 240 ˚C by TGA[16].

MIL-101: MIL represents Materials of Institut Lavoisier, a research institute of materials led by Gerard Ferey in France concentrating on the development of novel nanomaterials for gas storage and catalysis. With the topology of super-tetrahedron, MIL-101 possesses a three-dimensional crystalline structure, large pore sizes of 29 and 34 Å and an ultrahigh Langmuir surface area up to 5900 m^2/g. In addition, MIL-101 is completely stable under air atmosphere and was not altered when treated with water and various organic solvents at room temperature or under hydrothermal conditions. The stability of MIL-101 was also measured at 275 ˚C by TGA[17].

ZIF-8: With the formula of [$Zn(MeIM)_2$]$_n$ (Me= methyl, IM= imidazolate), ZIF-8, as the prototype of ZIF materials, has a three-dimensional crystalline structure with a zeolite-like topology. The ZIF-8 structure is composed of tetrahedral ZnN_4 units bridged with imidazolate links, giving a pore size of 11.6 Å (in diameter) and a small aperture of 3.4 Å (across). The apparent surface areas of ZIF-8 were estimated at 1810 m^2/g (Langmuir) and 1630 m^2/g (BET), respectively. In particular, the chemical and thermal stability of

ZIF-8 is outstanding among a large number of MOFs. According to the water stability tests, ZIF-8 was chemically stable in boiling water, alkaline solutions, and organic solvents without loss of crystallinity and porosity. The upper limit of thermal stability for ZIF-8 is up to 550 ˚C, obtained by TGA[18].
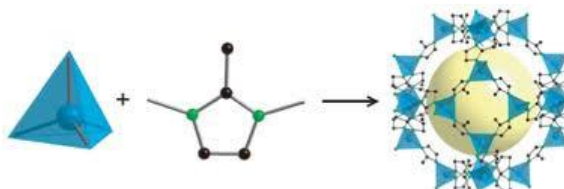
Figure 1.1 The 3-D Crystalline Structure of ZIF-8.
Source: http://www. ms.ucla.com

Ni(FA) and Zn(FA): Ni(FA) and Zn(FA) represent nickel formate, [$Ni_3(HCOO)_6$] ÐMF and zinc formate, [$Zn_3(HCOO)_6$] respectively. The family of porous materials, [$M_3(HCOO)_6$] (M= Mn, Fe, Co, Ni, Zn), possesses robust and flexible diamond framework based on M-centered tetrahedral nodes. The overall framework gives rise to the zigzag channels with the effective pore size of 5-6 Å. They display permanent porosity, stability for thermal treatment, a wide range of gas or liquid guest inclusion behavior and 3-D long-range magnetic ordering[19]. Ni(FA) has an appearance of light green crystalline powder and the thermal stability up to 275 ˚C obtained by TGA. It is well known that nickel is a commonly used metal catalyst in steam reforming and water gas shift reactions. Ni(FA), containing nickel, is expected to have potential in catalyzing the water gas shift reaction. Zn(FA) has an appearance of white crystalline powder and the thermal stability up to 250 ˚C obtained by TGA. Both the samples and related data were provided by Professor Li, Jing from The State University of New Jersey-Rutgers at New Brunswick.

Table 1.1 Summary of Properties of Several Typical MOFs

Category	Molecular Formula	Water Stability	Thermal Stability	Langmuir Surface Area(m^2/g)
MOF-5	$[Zn_4O(BDC)_3]_n$	minimally stable	450 ˚C[18]	> 2900
MOF-177	$[Zn_4O(BTB)_2]_n$	minimally stable		> 5000
HKUST-1	$[Cu_3(BTC)_2]_n$	Slightly stable	240 ˚C	> 900
MIL-101(Cr)	$[Cr_3F(H2O)_2O(BDC)_3]_n$	Completely stable	275 ˚C	~ 5900
ZIF-8	$[Zn(MeIM)_2]_n$	Completely stable	550 ˚C	~ 1800
Ni(FA)	$[Ni_3(HCOO)_6]$ ꞏDMF		275	
Zn(FA)	$[Zn_3(HCOO)_6]$		250	

Note: BDC= benzene-1, 4-dicarboxylate; BTB= benzene-1, 3, 5-tribenzoate;
BTC= 1, 3, 5-benzene-tricarboxylate; Me= methyl; IM= imidazolate.

1.4 Objective

Currently, most of the researches have been focused on developing new MOF structures and exploring their use in gas storage and separation. Only few studies investigated the catalytic properties of MOFs. The objective of this study is to investigate three MOF materials including zeolitic imidazolate framework-8 (ZIF-8), Ni(FA) and Zn(FA) and test their catalytic properties. In this study, ZIF-8 was employed as a catalyst support for preparing iron and platinum nanoparticle catalysts via incipient wetness impregnation method. These MOF materials and as-prepared catalysts were characterized by Brunauer-Emmett-Teller (BET), X-ray diffraction (XRD), temperature-programmed reduction (TPR), pulse chemisorption and temperature-programmed desorption (TPD). The catalysts were also tested for the water gas shift and methanol oxidation reactions using a fixed bed flowing reactor at 1 atm.

CHAPTER 2

SYNTHESIS OF CATALYSTS

2.1 Preparation of Fe-ZIF8

The metal salts $Fe(NO_3)_3$ $9H_2O$ (0.0149 g) were dissolved in deionized water (640 μL). The solution was impregnated dropwise onto the ZIF-8 powders (0.2665 g), which were calcined at 300 ˚C for 2 h. The resulting samples were dried at 110 ˚C for 12 h and calcined in air at 200 ˚C for another 3 h. The iron loading was 0.77 wt%.

2.2 Preparation of Pt-ZIF8

The precious metal salts $Pt(NO_3)_2$ $4NH_3$ (99% purity, 0.0019 g) were dissolved in deionized water (220 μL). The solution was impregnated dropwise onto the ZIF-8 powders (0.2675 g), which were calcined at 300 ˚C for 2 h. The resulting samples were dried at 110 ˚C for 12 h and calcined in air at 260 ˚C for another 3 h. The platinum loading was 0.35 wt%. Different loading with 2.1 wt% was prepared similarly. Two batches of 2.1 wt% Pt-ZIF8 were synthesized and calcined at 300 ˚C and 400 ˚C differently.

CHAPTER 3

CHARACTERIZATION

3.1   X-ray Diffraction

XRD was performed for the samples in powder form with a Philips PW 3040 X-ray diffractometer (Cu K_α radiation, 0.154 nm), operated at 45 kV/40 mA. The samples were analyzed in the 2θ range from 5 to 50° using a 0.1° step size with a 1-s dwell time at each step.

3.2   BET Analysis

BET analysis is a widely used multi-layer physisorption method to measure the total surface area of a solid material, usually at liquid nitrogen temperature, 77 K. During BET measurements, the analysis gas N_2 is instantly adsorbed on the sample at 77 K. When the sample returns to room temperature, the N_2 will desorb from the sample. Both the adsorption and desorption of the N_2 are recorded by thermal conductive detector (TCD) in Autochem II 2920. The amount of nitrogen desorbed and the sample weight are used to calculate the total specific surface area. In this study, a sample of about 30 mg was loaded in the quartz U-tube. After the pretreatment, the sample was cooled down to the ambient temperature. The analysis gas, 30% N_2 in He, was used flowing over the samples after the pretreatment. The N_2 was instantly adsorbed on the sample at 77 K and begun to desorb when the liquid nitrogen dewar was removed from the U tube. The adsorbed and desorbed N_2 was analyzed with a TCD detector and the signals were recorded with the on-line computer.

3.3 Temperature-Programmed Reduction (TPR)

TPR is a powerful tool to determine the number of reducible species (usually metal oxides) present in the catalyst and the corresponding reduction temperatures. TPR analysis is performed with a linear temperature ramp using a reducing gas, usually H_2 in an inert gas such as argon. If a reduction takes place at a certain temperature, the change of H_2 concentrations is recorded, giving the integrated H_2 consumption. In addition, TPR analysis can reveal the effect of the support and promoters on the reducibility of the catalyst. In this study, a gas mixture of 10% H_2 in Ar was used as the reducing agent and the flow rate was controlled at 50 cm^3/min by mass flow controller (MFC). The concentration of H_2 was recorded by mass spectrometer (MS, QMS 200, Stanford Research Systems).

3.3.1 TPR on Unmodified ZIF-8, 0.77 wt% Fe-ZIF8 and 0.35 wt% Pt-ZIF8

The unmodified ZIF-8 sample of 0.0148 g was placed in the quartz U-tube reactor. The sample was heated from room temperature to 800 ˚C with a constant ramp rate of 10 ˚C/min while the reducing gas, 10% H_2 in Ar, of 50 cm^3/min flew through the sample. The concentration of hydrogen was recorded over the whole temperature range by MS at the exit of Autochem II 2920. In addition, the similar procedures were also used for TPRs on the 0.77 wt% Fe-ZIF8 and 0.35 wt% Pt-ZIF8 samples.

3.4 Pulse Chemisorption

Pulse chemisorption determines the active surface area, metal dispersion and average active particle size on the supported catalyst by applying measured doses of reactant gas

(usually H_2 or CO) to the sample. The reactant gas reacts with each active site until all sites are saturated. The first few injections of reactant gas may be totally consumed. As the sites approaches saturation, peaks representing unreacted gas molecules appear and the injected gases will not be adsorbed anymore. The amount of reactant gas chemisorbed is the difference between the total amount of gas injected and the sum amount that did not react with the active sites of the sample. The amount of each pulse of reactant gas is determined by the loop volume on an automatically controlled valve. In this study, a mixture of 10% H_2 in Ar was used to provide the reactant gas, hydrogen. After the pretreatment, the sample was cooled down to room temperature and the analysis gas was dosed on the sample until saturation.

3.5 Temperature-Programmed Desorption (TPD)

Temperature-programmed desorption determines the number, type, and strength of active sites available on the surface of a catalyst by measuring the amount of gas desorbed at various temperatures. After the analysis gas is dosed on the sample until saturation, the gas desorption is run with a linear temperature ramp while an inert gas flows through the sample. At a certain temperature, the heat overcomes the bond energy between gas adsorbate and active site, hence the pre-adsorbed gases desorb from the sample. The volume of desorbed species, combined with the stoichiometry factor and the temperature at which pre-adsorbed species release, yields the number and strength of active sites. The number of desorption peaks can indicate the surface sites with the different bond energies; and the peak area represents the quantity of adsorbed species on a given active site.

3.5.1 H_2 TPD and CO_2 TPD on ZIF-8

The ZIF-8 sample of 0.0188 g, calcined at 300 ˚C, was loaded in the quartz U-tube reactor. Prior to hydrogen dosing, the sample was degassed using 50 cm^3/min helium at 200 ˚C for 30 min. After the pretreatment, the sample was cooled down to room temperature under helium and the analysis gas, 10% H_2 in Ar, was dosed on the sample for maximum 20 times. Following the hydrogen dosing, the hydrogen desorption was run with a linear temperature ramp of 15 ˚C/min to 600 ˚C while a steady stream of helium flew over the sample at 50 cm^3/min. The concentration of H_2 desorbed was recorded by MS at the exit of the exhaust line. In addition, the similar procedures were also used for CO_2 TPD on the same ZIF8 samples and the analysis was switched to CO_2.

3.5.2 H_2 TPD on 0.77 wt% Fe-ZIF8 and 0.35 wt% Pt-ZIF8

The Fe-ZIF8 sample of 0.0080 g, calcined at 200 ˚C, was placed in the quartz U-tube reactor. Before hydrogen dosing, the sample was reduced at 300 ˚C for 30 min using the reducing gas, 10% H_2 in Ar, of 50 cm^3/min. After the pretreatment, the sample was cooled down to room temperature under argon and the analysis gas, 10% H_2 in Ar, was injected on the sample for maximum 20 times. Following the hydrogen dosing, the hydrogen desorption was run by heating the sample to 600 ˚C at a constant rate of 15 ˚C/min while a stream of 50 cm^3/min helium flew over the sample. The concentration of H_2 desorbed was recorded by MS at the exit of the exhaust line. Similarly, these procedures were also tested on the 0.35 wt% Pt-ZIF8 samples.

CHAPTER 4

CATALYTIC REACTIONS

4.1 Methanol TPD without Oxygen on 0.35wt% Pt-ZIF8 and Ni(FA)

TPD of methanol is used to test the catalyst activity towards methanol decomposition. The Pt-ZIF8 sample of 0.0158 g, calcined at 260 ˚C, was loaded in the quartz U-tube reactor. Prior to methanol dosing, the sample was reduced at 200 ˚C for 30 min using the reducing gas, 10% H_2 in Ar, of 50 cm^3/min. After the pretreatment, the sample was cooled down to room temperature under argon and meanwhile the methanol solvent was vaporized and dosed on the sample through the injection loop for maximum 20 times. Following the methanol dosing, the methanol adsorbed on the sample begun to decompose from room temperature to 600 ˚C increased by 15 ˚C/min. The products including hydrogen, carbon monoxide, carbon dioxide, methane and water from the methanol decomposition were analyzed with a MS and recorded by an on-line computer. Similarly, these procedures were also used for the methanol TPD on Ni(FA).

4.2 Methanol TPD with Oxygen on 2.1 wt% Pt-ZIF8 (ZIF-8 300 ˚C), 2.1 wt% Pt-ZIF8 (ZIF-8 400 ˚C), Ni(FA) and 1 wt% Pt-ZIF8

TPD of methanol with oxygen is used to test the catalyst activity towards methanol oxidation. The Pt-ZIF8 sample of 0.0487 g, calcined at 260 ˚C, was loaded in the quartz U-tube reactor. Prior to methanol dosing, the sample was reduced at 200 ˚C for 30 min using the reducing gas, 10% H_2 in Ar, of 50 cm^3/min. After the pretreatment, the sample was cooled down to room temperature under argon and meanwhile the methanol solvent was vaporized and discretely dosed on the sample through the injection loop for maximum

20 times. Following the methanol dosing, the methanol adsorbed on the sample reacted with oxygen, which was provided by a stream of the analysis gas, 1% O_2 in He, of 50 cm^3/min. The reaction was run from room temperature to 600 ˚C at a ramp rate of 15 ˚C/min. The products including hydrogen, carbon monoxide, carbon dioxide, formaldehyde, methane and water from the methanol oxidation were analyzed by MS. Similarly, these procedures were also used for the methanol TPDs with O_2 on Ni(FA), 2.1 wt% Pt-ZIF8 (ZIF-8 400 ˚C) and 1 wt% Pt-CeO$_2$.

4.3   Water Gas Shift (WGS)

The WGS reaction was carried out at 1 atm in the fixed-bed reactor in which 0.1110 g Ni(FA) catalysts were used. Before the reaction, the catalysts were pretreated at 180 ˚C for 30 min using a steady stream of N_2 of 70 cm^3/min. After the pretreatment, the reactant gas, 10% CO in He, passed through the pre-heater and fed into the reactor at a flow rate of 103 cm^3/min. The other reactant water was pumped to the pre-heater for vaporization at a flow rate of 0.05 ml/min and introduced to the catalyst bed. The molar ratio of CO and H_2O was 1: 6. The reaction temperatures ranged from 180 to 250 ˚C, which is the upper limit of the stability for Ni(FA). The reactants and products were analyzed by gas chromatography (GC, Agilent 7890A GC System) using the TCD detector. Similarly, these procedures were also used for the 2.1 wt% Pt-ZIF8 (ZIF-8 300 ˚C) catalysts of 0.1050 g in the WGS reaction. The catalysts were reduced at 200 ˚C for 30 min before the reaction and the reaction temperatures ranged from 250 to 350 ˚C.

CHAPTER 5

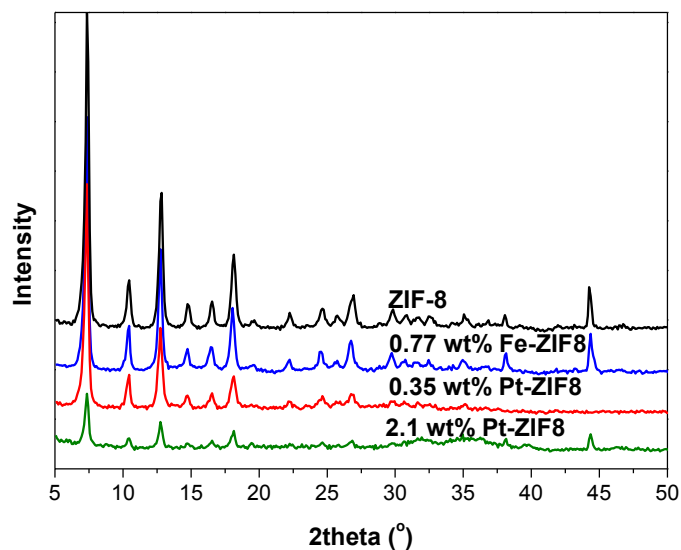# RESULTS AND DISCUSSION

5.1 XRD Analysis

Figure 5.1 X-ray Diffractograms of ZIF-8s (calcined at 300 ˚C).

Figure 5.1 shows that the ZIF-8 sample, calcined at 300 ˚C, maintains its crystal structure with clear diffraction peaks. After incorporating Fe and Pt with the different loadings, the crystallinity of ZIF-8 is still well-maintained in these samples. However, the peak intensities become much lower for the 2.1 wt% Pt-ZIF8 sample, which ZIF-8 was calcined at 300 ˚C. That's probably because the incorporated platinum nanoparticles made a slight change of the regularity of the ZIF-8 lattice structure.
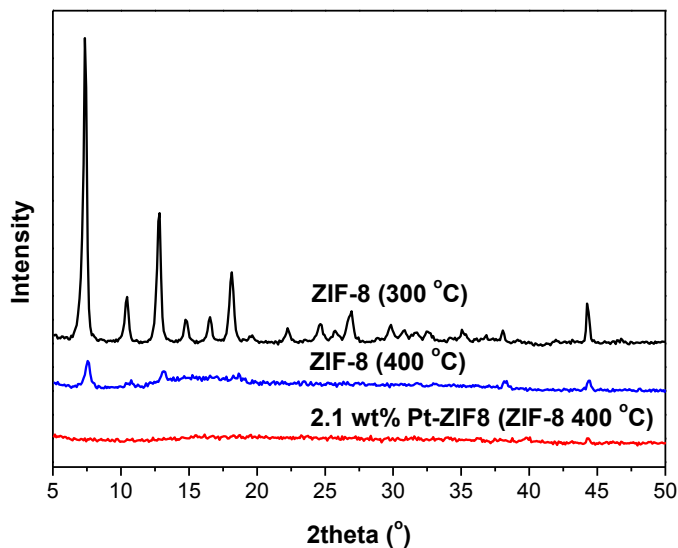
Figure 5.2 X-ray Diffractograms of ZIF-8s (calcined at 300 ˚C and 400 ˚C).

Figure 5.2 shows a huge difference in the crystallinity between the ZIF-8 samples calcined at 300 ˚C and 400 ˚C respectively. When the ZIF-8 sample was calcined at 400 ˚C, its crystal lattice structure collapsed. The reason why the collapse happened is that the organic species within the ZIF-8 structure underwent oxidation when calcined in air at 400 ˚C. It's not surprising that the 2.1wt% Pt-ZIF8 sample prepared over the ZIF-8 sample calcined at 400 ˚C shows a completely amorphous structure.
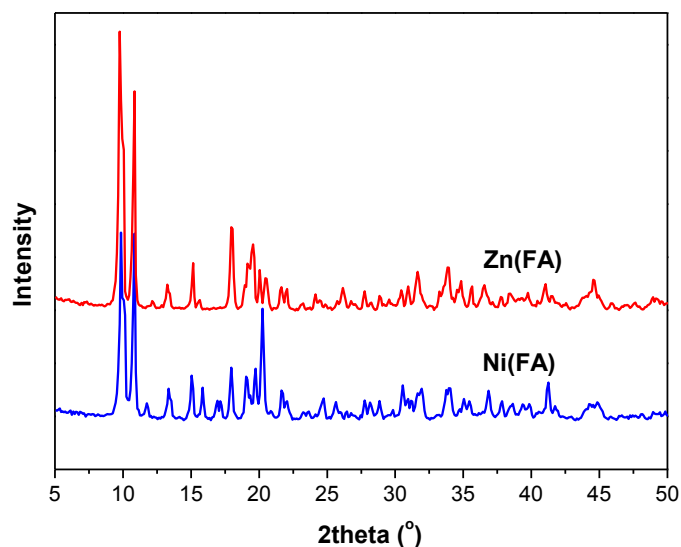
Figure 5.3 X-ray Diffractograms of Ni(FA) (calcined at 180 ˚C) and Zn(FA) (calcined at 150 ˚C).

For the Ni(FA) and Zn(FA) samples, the calcination temperatures were chose based on their thermal stability. Both of them maintain their crystal lattice structure well after calcined at 180 ˚C and 150 ˚C respectively (Figure 5.3).

Based on the XRD analysis above, the stability of these three samples are relatively low. For ZIF-8, the crystal lattice structure is well-maintained when calcined at 300 ˚C, but collapses when calcined at 400 ˚C. Both Ni(FA) and Zn(FA) maintain their crystal structures well after calcined at 180 ˚C and 150 ˚C respectively.

5.2 BET Analysis

Table 5.1 Summary of BET Surface Area Measurements (77 K)

Sample	BET surface area (m^2/g)
ZIF-8 (300 ˚C)	847
0.35 wt% Pt-ZIF8 (ZIF-8 300 ˚C)	700
0.77 wt% Fe-ZIF8	497

(ZIF-8 300 ˚C)	
2.1 wt% Pt-ZIF8	355
(ZIF-8 300 ˚C)	
ZIF-8 (400 ˚C)	62
2.1 wt% Pt-ZIF8	26
(ZIF-8 400˚C)	
Ni(FA) (180˚C)	244
Zn(FA) (150˚C)	18

The ZIF-8 sample, calcined at 300 ˚C, has a large BET surface area of 847 m^2/g. However, for the ZIF-8 sample calcined at 400 ˚C, the BET surface area dramatically decreases to 62 m^2/g. The big difference in the resulting surface areas is due to the structural collapse of ZIF-8 when calcined at 400 ˚C, which is consistent with the previous XRD spectra. In addition, the Ni(FA) sample calcined at 180 ˚C has a BET surface area of 244 m^2/g; but the Zn(FA) sample calcined at 150 ˚C has a very limited surface area of 18 m^2/g.
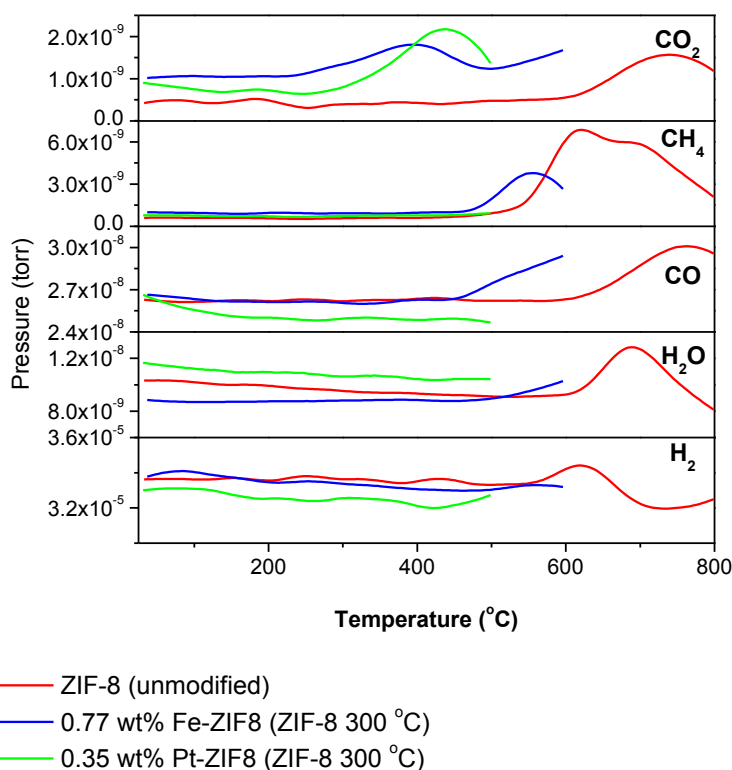
5.3   TPR Analysis

Figure 5.4 TPR on Unmodified ZIF-8, Activated 0.77 wt% Fe-ZIF8 and 0.35 wt% Pt-ZIF8.

Figure 5.4 shows that no hydrogen was consumed over the whole temperature range for the 0.77 wt% Fe-ZIF8 and 0.35 wt% Pt-ZIF8 samples during the TPRs. It's likely due to the low loadings of the incorporated Fe and Pt oxides. The other possibility is that their nanoparticles were covered by the support ZIF-8; hence the hydrogen did not react with these metal sites.

The release of other species at the temperature above 400 ˚C is related to the collapse of the ZIF-8 structure. For example, the methane is from the dissociation of the branched methyl of the imidazolate link and subsequent hydrogenation at around 500 ˚C.

The carbon monoxide and/or carbon dioxide is from the decarburization of the residual solvent molecules in the pores of ZIF-8 at high temperature.

5.4   Pulse Chemisorption

Table 5.2 Summary of Pulse Chemisorption Results (35 ˚C, 1 atm)

Sample	Cumulative H_2 adsorption quantity (μmol/g)	Metal Dispersion (%)
0.77 wt% Fe-ZIF8 (ZIF-8 300 ˚C)	2.70	4.1389
0.35 wt% Pt-ZIF8 (ZIF-8 300 ˚C)	0.36	4.0136
2.1 wt% Pt-ZIF8 (ZIF-8 400 ˚C)	1.67	3.1086

The cumulative number of hydrogen adsorbed on these three catalyst samples is extremely low, nearly zero. The analysis gas, 10% H_2 in Ar, did not react with the active metal sites. It's because most of these active metal sites were covered by the support ZIF-8, rather than distributed on the surfaces of ZIF-8. It also explains the low metal dispersions on the ZIF-8 surfaces.
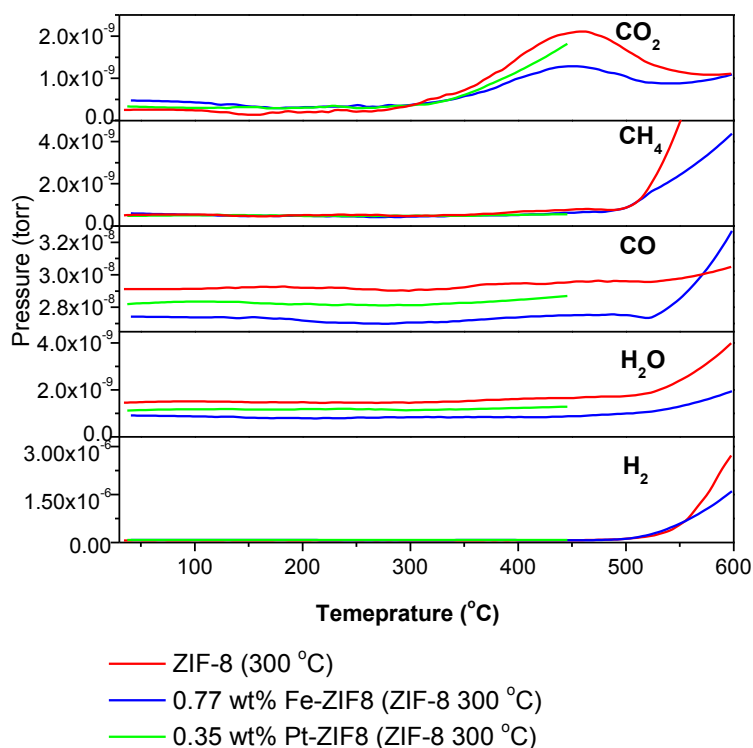
5.5 H_2 TPD

Figure 5.5 H_2 TPD on ZIF-8 (calcined at 300 ˚C), 0.77 wt% Fe-ZIF8 and 0.35 wt% Pt-ZIF8.

Based on the literature, there are two hydrogen adsorption sites present within the ZIF-8 structure. The first site is on top of the C=C double bond of the imidazolate link with an adsorption energy of 8.6 kJ/mol; the second one is at the central voids of the Zn hexagon with an adsorption energy of 6.2 kJ/mol. These adsorption energies are relatively low and the bonding between H_2 molecules and the adsorption sites is also weak. Currently, the significant hydrogen uptake for ZIF-8 was realized at cryogenic conditions [20].

During H_2 TPD, the cumulative quantity of hydrogen adsorbed on the ZIF-8 sample was extremely low, 3.45 µmol/g at 35 ˚C and 1 atm. The bond strength between hydrogen molecules and the adsorption sites is not strong enough to prevent hydrogen molecules

desorbing from the ZIF-8 sample. Figure 5.5 shows that the hydrogen desorbs from the ZIF-8 and 0.77 wt% Fe-ZIF8 samples at around 450 °C. Because both of them did not adsorb H_2 molecules during the H_2 dosing, the H_2 release is likely due to the structural collapse of ZIF-8 at above 400 °C, rather than desorption of the pre-adsorbed H_2 molecules. Similarly, the release of other species is also related to the structural collapse of ZIF-8 at high temperatures.
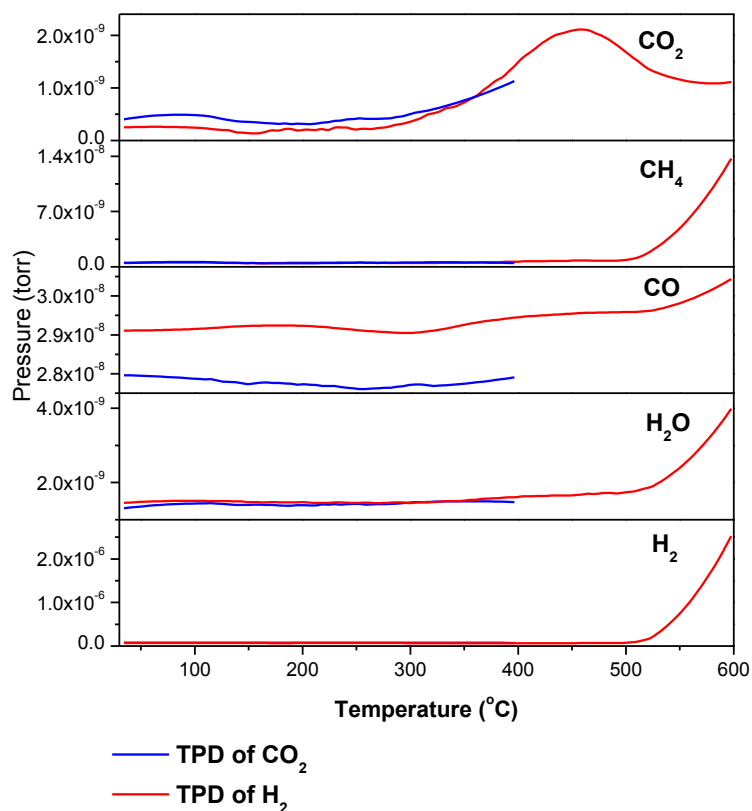
5.6 CO_2 TPD

Figure 5.6 H_2 TPD and CO_2 TPD on ZIF-8 (calcined at 300 °C).

During the CO_2 TPD, the cumulative quantity of CO_2 adsorbed on the ZIF-8 sample was nearly zero at 35 °C and 1 atm. In Figure 5.6, the CO_2 release at around 250 °C is possibly due to the decarburization of residual solvent molecules in the pores of ZIF-8,

rather than desorption of the pre-adsorbed CO_2 molecules. Again, that's because the ZIF-8 sample did not adsorb CO_2 molecules during the CO_2 dosing at 35 ˚C and 1 atm.
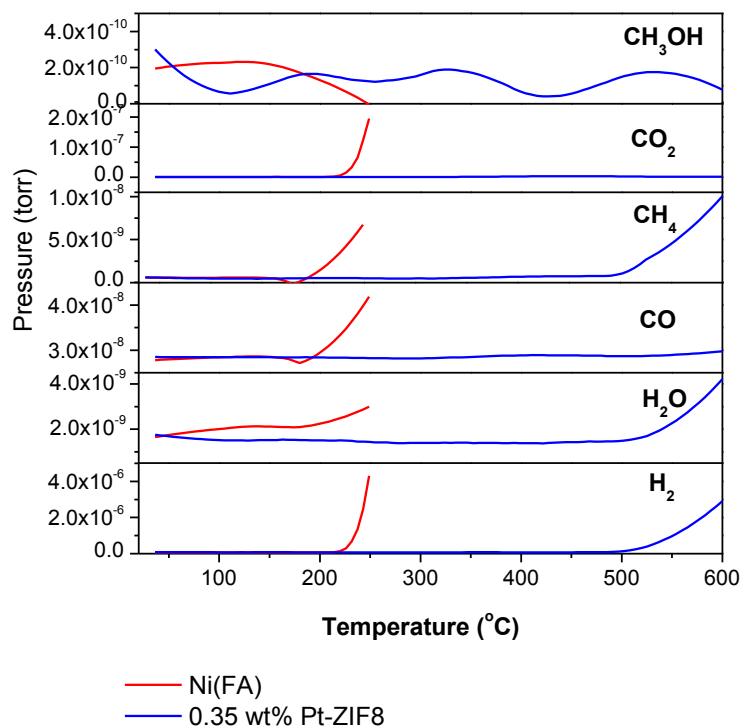
5.7 Methanol TPD without Oxygen

Figure 5.7 Methanol TPD without Oxygen on Ni(FA) and 0.35 wt% Pt-ZIF8.

Methanol TPD is used to test the catalyst activity towards the methanol decomposition. In the absence of oxygen, the methanol adsorbed on the Ni(FA) surfaces was thermally decomposed from room temperature to 250 ˚C, giving H_2 and CO_2 at 220 ˚C as well as minor CO and CH_4 at 175 ˚C. Similarly, the methanol adsorbed on the 0.35 wt% Pt-ZIF8 surfaces was thermally decomposed from room temperature to 600 ˚C. The products were obtained at above 500 ˚C, which exceeds the stability of ZIF-8, 400 ˚C. Compared to 0.35 wt% Pt-ZIF8, Ni(FA) has better potential in catalyzing the methanol

decomposition, which occurred at the lower temperature, below the upper limit of its stability.
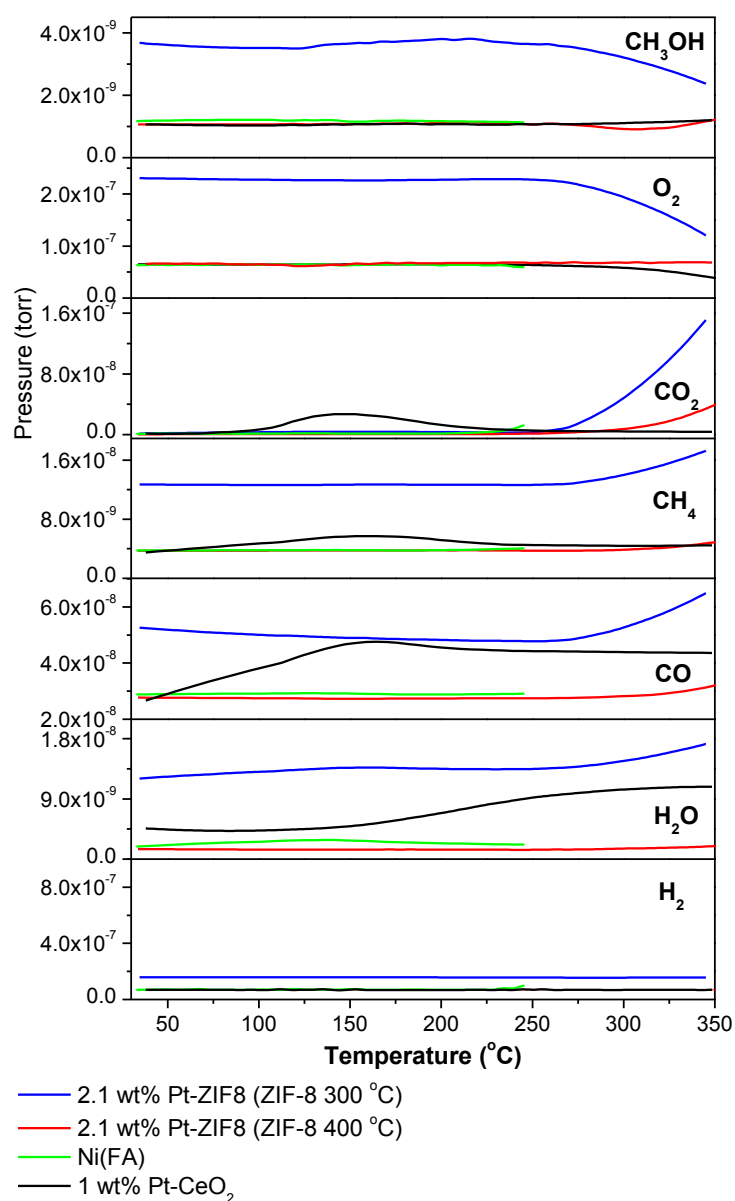
5.8   Methanol TPD with Oxygen

Figure 5.8 Methanol TPD with Oxygen on 2.1 wt% Pt-ZIF8 (ZIF-8 300 ˚C), 2.1 wt% Pt-ZIF8 (ZIF-8 400 ˚C), Ni(FA) and 1 wt% Pt-CeO$_2$.

Methanol TPD with oxygen is used to test the catalyst activity towards the methanol oxidation. Figure 5.8 shows that the methanol adsorbed on the 1 wt% Pt-CeO_2 catalysts underwent oxidation at below 100 ˚C, giving the main products CO and CO_2 as well as minor CH_4 and H_2O. For the 2.1 wt% Pt-ZIF8 samples (ZIF-8 300 ˚C), the dosed methanol was oxidized to produce the highest concentrations of CO and CO_2 as well as CH_4 and H_2O at 260 ˚C. Compared with these two catalysts, Ni(FA) and 2.1 wt% Pt-ZIF8 (ZIF-8 400 ˚C) have relatively low catalytic activities on the methanol oxidation. For the latter, it's mainly due to the low surface area of the support ZIF-8 when calcined at 400 ˚C, thereby decreasing the number of the active sites on the surfaces of ZIF-8. In summary, 1 wt% Pt-CeO_2 and 2.1 wt% Pt-ZIF8 (ZIF-8 300 ˚C) have better potential in catalyzing methanol oxidation reactions than Ni(FA) and 2.1 wt% Pt-ZIF8 (ZIF-8 400 ˚C).

5.9   Water Gas Shift

The WGS reactions were run for Ni(FA) and 2.1 wt% Pt-ZIF8 (ZIF-8 300 ˚C) in the fixed-bed reactor at 1 atm. Neither of the catalysts catalyzed the WGS reaction, because no H_2 and CO_2 products were detected by GC. Only the reactant water was collected at the bottom of the reactor. Both of them did not exhibit promising activities towards the WGS reaction, due to the low reaction temperatures limited by the stability of these MOF materials or the low metal dispersions on the MOF surfaces.

CHAPTER 6

CONCLUSION AND FUTURE PLANS

In this pioneering work, we investigated the catalytic activities of ZIF-8, Ni(FA) and Zn(FA) metal organic frameworks. These materials are rarely reported in the catalytic field. The author characterized and tested their activities towards clean hydrogen productions from water gas shift reaction and methanol partial oxidation. The characterization results show that these MOFs after incorporating Pt or Fe decompose at relatively low temperatures. The activities of these catalysts are much lower compared to the conventional catalyst systems. The reason is possibly due to the structural collapse during the reaction and the low metal dispersion on the MOF surfaces. Thus, future goal for applying these types of materials as catalysts is to maintain the structural stability of the MOFs during the real operation conditions and to investigate novel method to highly disperse metal atoms or nanoparticles on the surfaces of MOFs.

REFERENCES

1. Rowsell, J., Yaghi, O. M., "Metal-organic frameworks: a new class of porous materials" *Microporous and Mesoporous Materials* **73**, 3 (2004).

2. Meek, S. T., Greathouse, J. A., Allendorf, M. D., "Metal-Organic Frameworks: A Rapidly Growing Class of Versatile Nanoporous Materials" *Advanced Materials* **23**, 249 (2011).

3. Phan, A., Doonan, C. J., Uribe-Romo, F. J., Knobler, C. B., O'Keeffe, M., Yaghi, O. M., "Synthesis, Structure, and Carbon Dioxide Capture Properties of Zeolitic Imidazolate Frameworks" *Acc. Chem. Res.* **43**, 58 (2010).

4. Qiu, S., Zhu, G., "Molecular engineering for synthesizing novel structures of metal-organic frameworks with multifunctional properties" *Coord. Chem. Rev.* **253** , 2891 (2009).

5. Rosi, N. L., Eddaoudi, M., Kim, J., O'Keeffe, M., Yaghi, O. M., "Advances in the chemistry of metal-organic frameworks " *CrystEngComm* **4**, 401 (2002).

6. Cychosz, K. A., Matzger, A. J., "Water Stability of Microporous Coordination Polymers and the Adsorption of Pharmaceuticals from Water" *Langmuir* **26**, 17198 (2010).

7. Küsgens, P., Rose, M., Senkovska, I., Fröde, H., Henschel, A., Siegle, S., Kaskel, S., "Characterization of metal-organic frameworks by water adsorption" *Microporous and Mesoporous Materials* **120**, 325 (2009).

8. Rowsell, J. L. C., Yaghi, O. M., "Strategies for Hydrogen Storage in Metal-Organic Frameworks" *Angew. Chem. Int. Ed.* **44**, 4670 (2005).

9. Meilikhov, M., Yusenko, K., Esken, D., Turner, S., Van Tendeloo, G., Fischer, R. A., "Metals@MOFs - Loading MOFs with Metal Nanoparticles for Hybrid Functions" *European Journal of Inorganic Chemistry* **2010**, 3701 (2010).

10. Hermes, S., Schröter, M.-K., Schmid, R., Khodeir, L., Muhler, M., Tissler, A., Fischer, R. W., Fischer, R. A., "Metal@MOF: Loading of Highly Porous Coordination Polymers Host Lattices by Metal Organic Chemical Vapor Deposition" *Angew. Chem. Int. Ed.* **44**, 6237 (2005).

11. Jiang, H., Liu, B., Akita, T., Haruta, M., Sakurai, H., Xu, Q., "Au@ZIF-8: CO Oxidation over Gold Nanoparticles Deposited to Metal-Organic Framework" *J. Am. Chem. Soc.* **131**, 11302 (2009).

12. Li, H., Eddaoudi, M., O'Keeffe, M., Yaghi, O. M., "Design and synthesis of an exceptionally stable and highly porous metal-organic framework" *Nature* **402**, 276 (1999).

13. Furukawa, H., Miller, M. A., Yaghi, O. M., "Independent verification of the saturation hydrogen uptake in MOF-177 and establishment of a benchmark for hydrogen adsorption in metal–organic frameworks" *Journal of Materials Chemistry* **17**, 3197 (2007).

14. Proch, S., Herrmannsdörfer, J., Kempe, R., Kern, C., Jess, A., Seyfarth, L., Senker, J., "Pt@MOF-177: Synthesis, Room-Temperature Hydrogen Storage and Oxidation Catalysis" *Chemistry - A European Journal* **14**, 8204 (2008).

15. Bordiga, S., Regli, L., Bonino, F., Groppo, E., Lamberti, C., Xiao, B., Wheatley, P. S., Morris, R. E., Zecchina, A., "Adsorption properties of HKUST-1 toward hydrogen and other small molecules monitored by IR" *Physical Chemistry Chemical Physics* **9**, 2676 (2007).

16. Chui, S. S. Y., Lo, S. M. F., Charmant, J. P. H., Orpen, A. G., Williams, I. D., "A chemically functionalizable nanoporous material [Cu$_3$(TMA)$_2$(H$_2$O)$_3$]$_n$" *Science (Washington, D. C.)* **283**, 1148 (1999).

17. Ferey, G., "A Chromium Terephthalate-Based Solid with Unusually Large Pore Volumes and Surface Area" *Science* **309**, 2040 (2005).

18. Park, K. S., Ni, Z., Cote, A. P., Choi, J. Y., Huang, R., Uribe-Romo, F. J., Chae, H. K., O'Keeffe, M., Yaghi, O. M., "Exceptional chemical and thermal stability of zeolitic imidazolate frameworks" *Proc. Natl. Acad. Sci. U. S. A.* **103**, 10186 (2006).

19. Wang, Z., Zhang, B., Zhang, Y., Kurmoo, M., Liu, T., Gao, S., Kobayashi, H., "A family of porous magnets, [M$_3$(HCOO)$_6$] (M=Mn, Fe, Co and Ni)" *Polyhedron* **26**, 2207 (2007).

20. Assfour, B., Leoni, S., Seifert, G., "Hydrogen Adsorption Sites in Zeolite Imidazolate Frameworks ZIF-8 and ZIF-11" *J. Phys. Chem. C* **114**, 13381 (2010).